A NEW MODELING APPROACH FOR A PRIORI UNCERTAINTIES OF LASER TRACKER ANGLE MEASUREMENTS

Peter E. Manwiller, M.Eng., P.E.
Particle Accelerator Alignment Engineer
Facility for Rare Isotope Beams (FRIB), Michigan State University East Lansing, MI 48824 USA.
ORCID: https://orcid.org/0000-0001-8582-5789
Email: manwille@frib.msu.edu

Author Keywords: Uncertainty modeling; Laser tracker; Network Adjustment; Maximum Permissible Error (MPE); Error propagation; Azimuth angle; Zenith angle

Abstract

Methods for modeling the uncertainty in laser tracker angle measurements vary within the metrology industry, leading to confusion and questionable stochastic modeling for survey network adjustments and error propagation analysis. Interpreting the published laser tracker manufacturer performance specifications to determine an a priori sigma value for weighting azimuth and zenith angle measurements can be confusing and has led to differing implementations. This paper proposes a unique way to model survey network a priori laser tracker angular uncertainties based on laser tracker manufacturers' published maximum permissible error (MPE) values referenced to ISO and ASME standards for weighting survey network measurements. This paper's proposed model takes into account the disparate effects that pointing errors, target centering errors, and leveling errors have on azimuth and zenith angular uncertainties for measurements with steep sightings and at near ranges.

Introduction

The one-sigma accuracy of a distance measurement (σ_D) is well understood to be range dependent; accuracy decreases with range. It is common practice to assume a ppm scaling term when modeling σ_D values. However, a typical default setting in metrology software applies a simplistic modeling of azimuth and zenith angle uncertainties (σ_α and σ_β respectively) by assuming that they are constant (i.e. not range dependent) (Hexagon Metrology, 2021). Another common assumption is that σ_α is equal to σ_β. However, by closely examining the sources of error in measuring azimuth and zenith angles, it will be shown in this paper that these assumptions of angular uncertainties are not valid. These

assumptions are especially tenuous for measurements that are steep or at near ranges due to the effects of pointing errors and target centering errors on angular accuracy. Also, because of the nature of angular measurements in a spherical coordinate system, the uncertainty of measured azimuths varies as a function of the zenith angle. Specifically, for a given slope distance, the azimuth uncertainty increases as the zenith angle moves higher or lower away from the instrument's horizontal plane (Dorsey-Palmateer, 2018).

Correctly modeling angular uncertainties gives the proper foundation for understanding how angular errors propagate to calculated coordinate values of measured points and provides a valid stochastic weighting model for least squares adjustment of survey networks. This paper proposes a unique way to model the uncertainty of laser tracker angles as a function of range and steepness. This paper will also demonstrate how different angular uncertainty models propagate to the uncertainty of the calculated coordinates of measured points. The focus of this paper evaluates laser tracker survey network measurements which assumes the reflector is stationary during observation. Thomas Ulrich published a dissertation covering the modeling of uncertainty for dynamic targets (Ulrich, 2016).

Sources of Angle Measurement Error

There are several sources of error to consider for azimuth and zenith measurements. There is always a small error present in reading the angular encoder circle. Also, there is a small error in pointing the optical axis to coincide with the center of the target. Target centering error is a third source of error. For laser tracker measurements using spherically mounted retroreflector (SMR) targets, the primary sources of target centering error come from the manufacturing errors of an SMR's sphericity and miscentering of the reflector optics inside the SMR. The vertex of the reflecting open-air corner cube of an SMR is nominally manufactured to be coincident with the center of the sphere. A typical 1.5-inch-diameter SMR has a sphericity of roughly 3 µm and an optical centering accuracy ranging from roughly 3 µm to 12 µm depending on the manufacturer's specified grade (MetrologyWorks, 2022). Other SMR characteristics such as optical flatness, optical reflectivity, and dihedral angle errors also affect the accuracy of the target (FARO Technologies, Inc., 2016). Sphericity and reflector centering errors are

systematic if the orientation of the SMR is maintained to a particular laser tracker position. However, points measured from multiple laser tracker positions for a survey control network (the scenario considered in this paper) will realize sphericity and reflector centering errors as random errors.

Instrument setup errors associated with forced centering over a point can also contribute to the total angular error (Ghilani, 2010). However, for laser tracker measurements, the instrument setup position and orientation are typically parameterized and solved with free stationing. Free stationing removes instrument setup errors from contributing to the total error of angular measurements (Manwiller, 2020).

Some laser trackers include a dual-axis inclination sensor that detects the deflection angle between gravity and the standing axis of the instrument. Some trackers with an inclinometer apply compensating corrections to the raw azimuth and zenith angles to improve the effective levelness of the instrument's setup. Assuming the laser tracker is perfectly leveled can be very useful because it reduces the number of free stationing parameters from 6 to 4. The uncertainty of inclinometer readings, if applied as compensations to azimuth and zenith angles, is another source of error. The azimuth angles of steep measurements are greatly affected by leveling errors (Anderson & Mikhail, 1998) which is something well-known in the context of astronomical observations (Ghilani, 2010). In chapter 7.8 of *Adjustment computations spatial data analysis 5th ed.,* Ghilani derived the contribution of the error to an azimuth observation (e_{α_L}) from a leveling error (e_L) observed at a given zenith angle (β) as the following:

$$e_{\alpha_L} = e_L cot(\beta) \quad (1)$$

Laser trackers that apply inclinometer compensation will measure azimuth angles with noticeably worse repeatability at steep angles as shown later in this paper. For steep measurements, leveling errors impact azimuth angle accuracy by an order of magnitude greater than zenith angle measurements. For steep measurements, the $cot(\beta)$ term becomes a large multiplier; as β approaches 0°, the $cot(\beta)$ multiplier term approaches infinity. Because azimuth angle accuracy for steep sightings is extremely sensitive to leveling errors, the accuracy of any inclinometer corrections will be incorporated into the

modeling of azimuth uncertainty in this paper as shown in Eq. 9. The large impact of leveling errors on azimuth accuracy for steep surveys is a common consideration in monitoring the top crest of embankment dams (Ogundare, 2015).

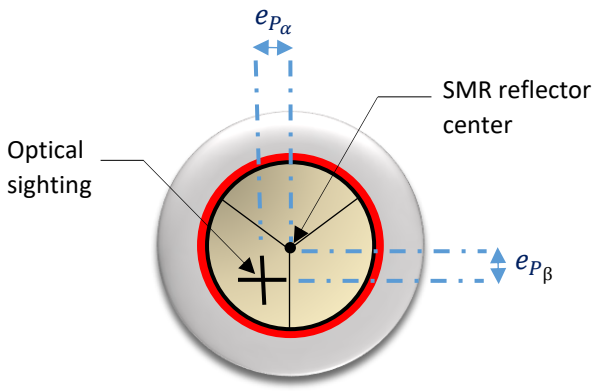

Fig. 1. *e_{P_α} and e_{P_β} components of optical pointing error*

Angle measurement error sources can be categorized as either random or systematic. Sources of systematic errors can arise from an uncalibrated instrument or from varying air conditions that create refracted nonlinear sight paths from the instrument to the reflector. Small geometric offsets, tilts, and eccentricities in the construction of a laser tracker can produce systematic errors in the angles and range readings if not properly compensated with an on-board software modeling of the errors and calibration (Muralikrishnan, et al., 2009). Assuming a well-calibrated instrument and stable environmental conditions free of systematic errors, the variance of an azimuth or zenith angle measurement $({\sigma_\theta}^2)$ will be equal to the sum of the angular variances of random errors associated with the following:

1) Electronic reading of the angular encoder $({\sigma_R}^2)$
2) Pointing the laser tracker's optic axis onto the center of the target $({\sigma_P}^2)$
3) Sphericity and reflector centering of the SMR target $({\sigma_T}^2)$

$${\sigma_\theta}^2 = {\sigma_R}^2 + {\sigma_P}^2 + {\sigma_T}^2 \quad (2)$$

If inclinometer corrections are applied to the observation, an additional parameter $({\sigma_L}^2)$ is included for azimuth observations as described later in this paper in Eq. 9.

A pointing error, e_P, associated with σ_P for a laser tracker's angular measurement can be modeled as a linear transverse offset from where the optic axis is pointing on the reflector to the true optical center of the reflector as shown in Fig. 1.

The pointing error results from the laser beam not perfectly locked onto the center of the SMR. The horizontal component of the pointing error (e_{P_α}) contributes to the total horizontal angular error. Likewise, the vertical component of the pointing error (e_{P_β}) contributes to the total vertical angular error. Laser trackers have an automatic target recognition (ATR) system to automatically center the optical axis onto the center of a reflective target. ATR helps remove the human variability of pointing errors that once relied on an operator's eyesight, but the pointing error is still inherent to the angle observation whether done by human sighting or using ATR. Chapter 4 of *Precision Surveying: The Principles and Geomatics Practice* discusses the physical conditions that contribute to pointing errors (Ogundare, 2015).

Because σ_P and σ_T represent lateral offset errors, their magnitude in angular terms is larger for nearer-range measurements. In other words, lateral offset errors have an equal effect on measuring a point's coordinates (X, Y, Z) at any range, but have a larger effect on the standard errors of angles at shorter distances. This means that angles observed at short distances are subject to more error and should be weighted accordingly (Ghilani, 2016). The following is the full quote from Ghilani:

> We can see that short sight distances result in larger overall errors in the angles even though the miscentering error is the same. That is: in terms of the point's coordinates, shorter sight distances have little effect on the coordinates of the stations but larger effects on the standard errors for the angles, which means that angles observed with short sight distances are subject to more error and should be weighted as such.

Therefore, the total contribution of angular uncertainty by σ_P and σ_T is increasingly less significant with increased range. It has been demonstrated in laboratory testing that a Leica LTD500 laser tracker's angular errors are dominated by lateral errors from σ_P and σ_T at a range of less than 2.5 meters (Meid & Sandwith, 2000). For ranges beyond roughly 2.5 meters (likely varying only slightly between laser trackers of other models), the electronic reading uncertainty of the angular encoders (σ_R) becomes the primary source of angular uncertainty.

Laser Tracker Manufacturer Accuracy Specifications

Laser tracker manufacturers specify the accuracies of their instruments in terms of maximum permissible error (MPE) according to ASME B89.4.19-2006 which is the American Society of Mechanical Engineer's standard for the performance evaluation of laser-based spherical coordinate measurement systems (ASME, 2006). The International Organization for Standardization (ISO) also provides a similar standard for testing and publishing laser tracker MPE values in the ISO 10360-10 specification (ISO, 2021). The specific ASME and ISO standards for laser trackers are important to reference for interpreting and testing laser tracker MPE values, because within the broader metrology industry (e.g. CMM machines) there are different standards for determining MPEs (Thompson, et al., 2021). Reported laser tracker MPE values cite either the ASME or ISO standard that was used for testing. Published laser tracker angular MPE values represent the extreme values of an error permitted by the specifications and are commonly interpreted to be roughly equivalent to a 3-sigma value of the laser tracker's angular performance (Leica Geosystems, 2009). Leica Geosystems states that "Unless stated otherwise, all accuracies are Maximum Permissible Error (≈ ±3 σ), with typical accuracies being ½ MPE (or approximately ±1.5 σ)" (Leica Geosystems, 2009). One published empirical test determined the distance uncertainties of three tested laser trackers to be smaller than their corresponding MPE specifications by at least a factor of four (Wang, Muralikrishnan, Hernandez, Shakarji, & Sawyer, 2020). Manufacturers commonly include alongside their instrument's published MPE value a "typical accuracies" value which is half the MPE value (FARO Technologies, Inc., 2016).

Understanding how to interpret these MPE values is important because they are the published accuracy performance values available for reference when considering purchasing a particular laser tracker model. A particular laser tracker passes each of the 41 distinctly configured ISO 10360-10:2021 laboratory test positions if, for each test position, 25 measurements are taken within the published MPE tolerances compared to a calibrated test length. However, if the errors in any of the 25 measurements exceed the MPE tolerance, three new measurements are permitted to be taken, of which the one with

the most error of the three can serve as a replacement. No more than two such replacements are permitted for ISO acceptance (ISO, 2021).

MPE values for angular performance are expressed in terms of the maximum permissible transverse error in micrometers (e_T). The transverse error is the error "resulting from incorrectly determining the angular components in determining the location of a measured point" (ISO, 2021). Therefore, the e_T value incorporates all sources of random errors (and residual systematic errors after calibration) including uncertainties associated with the angular encoder reading (σ_R), ATR optical pointing (σ_P), target centering (σ_T), and leveling (if applicable) (${\sigma_L}^2$). This is why e_T is commonly published by manufacturers with the stipulation that their most precise instrument measurement mode and highest grade SMRs be used for testing (Hexagon Metrology, 2012).

Angular transverse MPE values are modeled based on the transverse error e_T formula shown in Eq. 3 as specified in Annex D of ISO 10360-10.

$$e_T\ (\mu m) = A_T\ (\mu m) + B_T\ (\mu m/m)\ R \tag{3}$$

Where A_T is a constant value expressed in micrometers and B_T is a dimensionless constant value multiplied by the range (R) between the tracker and the point being measured. Manufacturers commonly publish their e_T MPE formula in their technical specification data sheets by representing B_T as a ratio of micrometers per meter. This paper proposes associating the ISO transverse error formula variables in Eq. 3 with the primary error sources of laser tracker angle measurements. Specifically, the A_T term is most closely associated with the combined linear transverse offset errors of σ_P and σ_T, and B_T is most closely associated with σ_R. These associations are further explained in the following example of a Leica AT400 series laser tracker.

Leica AT400 series laser trackers have a published value of 1-sigma angular encoder reading accuracy (σ_R) of 0.5 arcseconds which is approximately $2.4\ \mu m/m$ (Leica Geosystems, 2010). The stated MPE for angular performance is $15\ \mu m + 6\ \mu m/m$ (Hexagon Metrology, 2018). The B_T term in Eq. 3 is primarily related to the uncertainty of the angular encoder reading (σ_R). Given a 1-sigma encoder reading accuracy of $2.4\ \mu m/m$, it follows that the Leica AT400 series tracker's B_T value ($6\ \mu m/m$) is

close to 3 times larger to represent the maximum permissible error. Similarly, the A_T value $(15\ \mu m)$ is closely related to the combined uncertainties of σ_P and σ_T because these are offset errors that become less angularly significant for longer-range measurements. Also, Leica AT400 series laser trackers have an inclinometer with a one-sigma accuracy (σ_L) of 0.5 arcseconds (Hexagon Metrology, 2012).

The values A_T and B_T in Eq. 3 represent a simplified linearized MPE modeling of the underlying sources of uncertainty propagated from σ_R, σ_P, and σ_T that contribute to the total uncertainty of σ_θ. The simple linear model in Eq. 3 is assumed to perform well enough at the typical ranges tested by the ISO and ASME standards which is implied to be beyond roughly 1.5 meters (ISO, 2021). However, a better model for observations at near ranges would recognize that A_T and B_T are approximations of two types of independent sources of uncertainty that would be more appropriately handled by applying principles of uncertainty propagation to combine the related terms a and b in quadrature shown in Eq. 4.

$$e_T\ (\mu m) = \sqrt{(a\ (\mu m))^2 + (b\ (\mu m/m)\ R)^2} \tag{4}$$

A similar treatment of converting linear specifications to a quadratic form is explained in the context of distance measurements by Ghilani in Eq. 7.38 of *Adjustment Computations Spatial Data Analysis* (Ghilani, 2010).

To relate the a and b terms to the A_T and B_T values provided by the manufacturer, let

$$a = \sqrt{{A_T}^2 + 3A_T B_T} \tag{5}$$

$$b = B_T \tag{6}$$

Defining a in Eq. 5 sets the quadratic form in Eq. 4 equal to the linear form in Eq. 3 at $R = 1.5\ m$ which is considered at the close range for testing laser tracker accuracy. Eq. 6 holds b equal to B_T to maintain the parity of linear and quadratic models for longer-range measurements where the angular contribution of A_T is negligible.

Fig. 2 compares how the transverse error (e_T), expressed as a transverse offset in micrometers, increases with range consistent in both the linear model (Eq. 3) and the quadratic model (Eq. 4). Fig. 2 also compares how the angle subtending the transverse error, in arcseconds, decreases as it approaches the arcseconds equivalent of the B_T value for both the linear and quadratic model. At the near range of 1.5 meters, the dominant effect on angular accuracy is the A_T term. At farther ranges, the A_T term becomes negligible and the angular accuracy becomes approximately constant, range independent, and dominated by the accuracy of the angular encoder reading (σ_R). Fig. 2 demonstrates how the calculated MPE angle is comparable between the standard linear model and this paper's proposed quadratic model for the ranges typically tested by the ISO and ASME standards. However, the quadratic model deviates from the linear model for ranges shorter than 1.5 meters by emphasizing the contribution of transverse uncertainties from σ_P and σ_T.

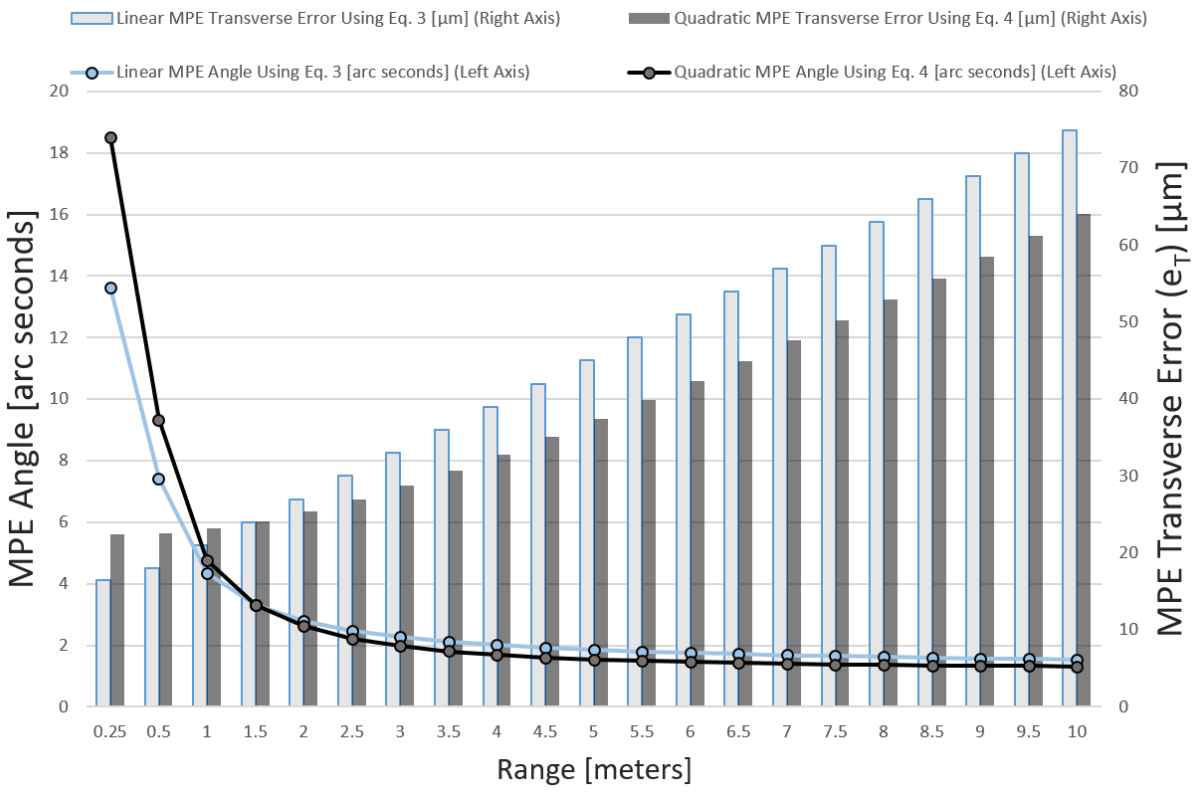

Fig. 2. *Leica AT400 series laser tracker MPE transverse error and angle as a function of range* $(A_T = 15\ \mu m, B_T = 6\ \mu m/m, a = 22\ \mu m, b = 6\ \mu m/m)$

Modeling Angular Accuracy Based on MPE Formulas

Given a laser tracker's A_T and B_T values provided by the manufacturer, consistent with Eq. 3, and determining a and b values consistent with quadratic modeling of transverse errors described in

Eqs. 4-6, this paper proposes unique formulas to estimate a priori 1-sigma uncertainties for azimuth and zenith angles (σ_α and σ_β) as a function of range (R) and zenith angle (β). Using the small angle approximation (dividing a and b terms by R to express transverse errors in angular radian terms) the equation for σ_β is the following:

$$\sigma_\beta\ (rad) = \sqrt{\frac{a(\mu m)}{3{,}000{,}000\ R(m)}^{\,2} + \frac{b\left(\frac{\mu m}{m}\right) R(m)}{3{,}000{,}000\ R(m)}^{\,2}} \tag{7}$$

Which simplifies to

$$\sigma_\beta\ (rad) = \sqrt{\frac{a(\mu m)}{3{,}000{,}000\ R(m)}^{\,2} + \frac{b\left(\frac{\mu m}{m}\right)}{3{,}000{,}000}^{\,2}} \tag{8}$$

Where R is the range (i.e. slope distance) from the tracker to the reflector, and the divisor 3 scales the MPE values (which approximate 3-sigma values) to 1-sigma. Notice that the a term must be converted from a distance unit to radians by diving by the range. The units given for the b term ($\mu m/m$) are a unitless microradian value that does not need to be scaled as a function of range as shown in Eq. 8. This makes sense because the angular accuracy of the encoder reading (σ_R) is unaffected by the range, which is the primary contributor to the b term.

For measurements that include leveling corrections, the published MPE values are expected to have considered all error sources including those from the instrument's reading of the inclination. Therefore, adding an inclination term to Eqs. 7 and 8 for zenith uncertainty would be considering the error twice and would be double counting. Leveling errors have the same small amount of effect on zenith angle uncertainty regardless of the steepness of observation (Ogundare, 2015). However, for steep observations, leveling errors impact azimuth angles by an order of magnitude greater than would be considered by the normal ISO and ASME testing ranges. This effect is reflected in Eq. 1. The multiplier factor of $cot(\beta)$ at $\beta = 5°$ is 11.4! Because ISO and ASME evaluations do not test at such steep angles, this effect on azimuth angles would not be reflected in the MPE values. This is why this paper proposes including a leveling term for the azimuth angle uncertainty formula in Eq. 9, but not for the zenith angle uncertainty formula in Eqs. 7 and 8.

The proposed equation for σ_α (Eq. 9) is similar to σ_β, but it uses the horizontal distance instead of the slope distance to convert the a term into radians by including $\sin(\beta)$ in the denominator. Also, the inclinometer uncertainty term (σ_L) is included, if applicable, as described in Eq.1.

$$\sigma_\alpha\,(rad) = \sqrt{\left(\frac{a(\mu m)}{3{,}000{,}000\ \sin(\beta)\ R(m)}\right)^2 + \left(\frac{b\left(\frac{\mu m}{m}\right)}{3{,}000{,}000}\right)^2 + \left(\sigma_L\,(rad)\ cot(\beta)\right)^2} \quad (9)$$

Using the horizontal distance to convert the a term to radians is necessary for calculating σ_α because horizontal offset errors of an azimuth angle are subtended by an arc with a radius equal to the measurement's horizontal distance. This is especially apparent at steep angles. To illustrate this, a 19.05 mm (0.75 inches) diameter U.S. penny held horizontally at arm's length (0.7 m) subtends roughly 1.5° of a viewer's horizontal viewing angle as shown in Fig 3. If held at arm's length 80° above horizontal, the penny subtends 9° of horizontal viewing angle. A penny held at arm's length above a viewer's head will subtend the full 360° of the viewer's horizontal angular viewing because the horizontal distance to the penny is zero once it is directly overhead. This illustrates why an azimuth measurement's horizontal offset errors are much larger, in angular terms, for steeper measurements.

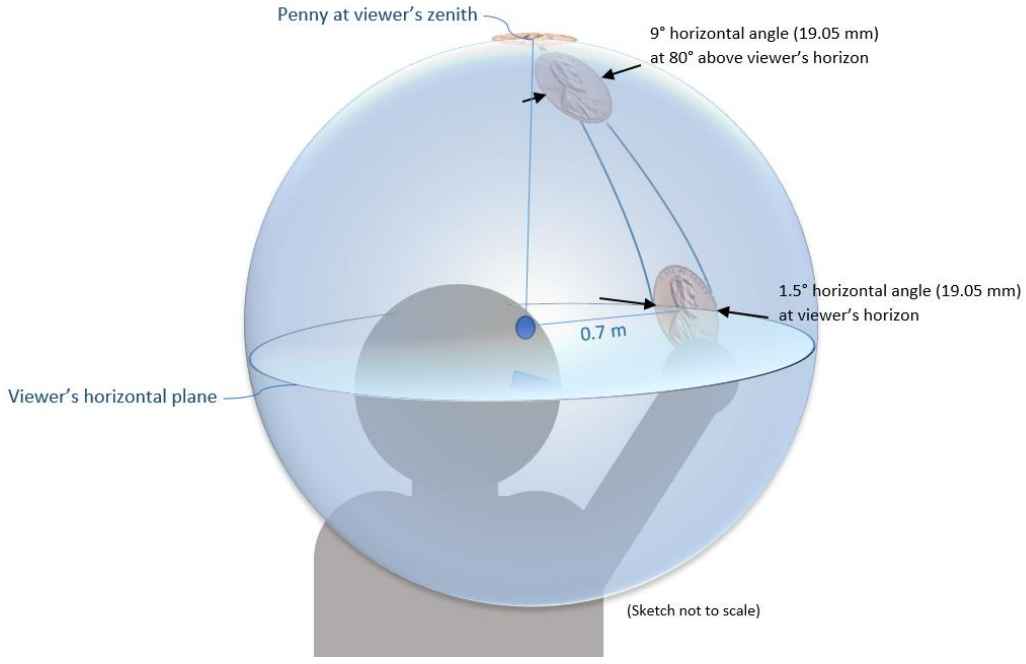

Fig. 3. *Horizontal viewing angle subtended by a penny at varying elevations*

The azimuth angle of an observation defines the direction of the horizontal distance. Increasingly steeper observations will have shorter horizontal distances which will increase the azimuth

angle's uncertainty. If an observation is so steep that the horizontal distance is shorter than the combined uncertainties from lateral offset errors (σ_P and σ_T) then the azimuth angle becomes unstable and nearly meaningless. This scenario is akin to attempting to report the longitude position of the North Pole. This effect is reflected in Eq. 9, where σ_α is undefined at β = 0°. It is also undefined at β = 180°, but this scenario is not relevant since the author is unaware of existing laser trackers that can peer downward through their own bodies. There are several models of trackers on the market that have either a removable handle or a curved handle to permit vertical viewing. Because the formula for calculating σ_α proposed in this paper (Eq. 9) utilizes the small angle approximation, the formula should be adapted to use the arctangent function for observations with extremely short horizontal distances. For observations pointing at (or very near) the zenith, the horizontal distance will become shorter than the combined uncertainties from the lateral offset errors (σ_P and σ_T), and the value of σ_α will become too large to provide stochastic value to the strength of a survey network. Before the indeterminacy of the σ_α value at the zenith is encountered, the azimuth observation can be stochastically ignored by down-weighting it completely. In this unique case, the value of an azimuth angle is understood to approach a uniform distribution where any value is equally likely between 0° and 360°.

Fig. 4 plots Eq. 9 using a and b values resulting from Leica's published A_T and B_T values for the AT400 series laser tracker at four different zenith angles.

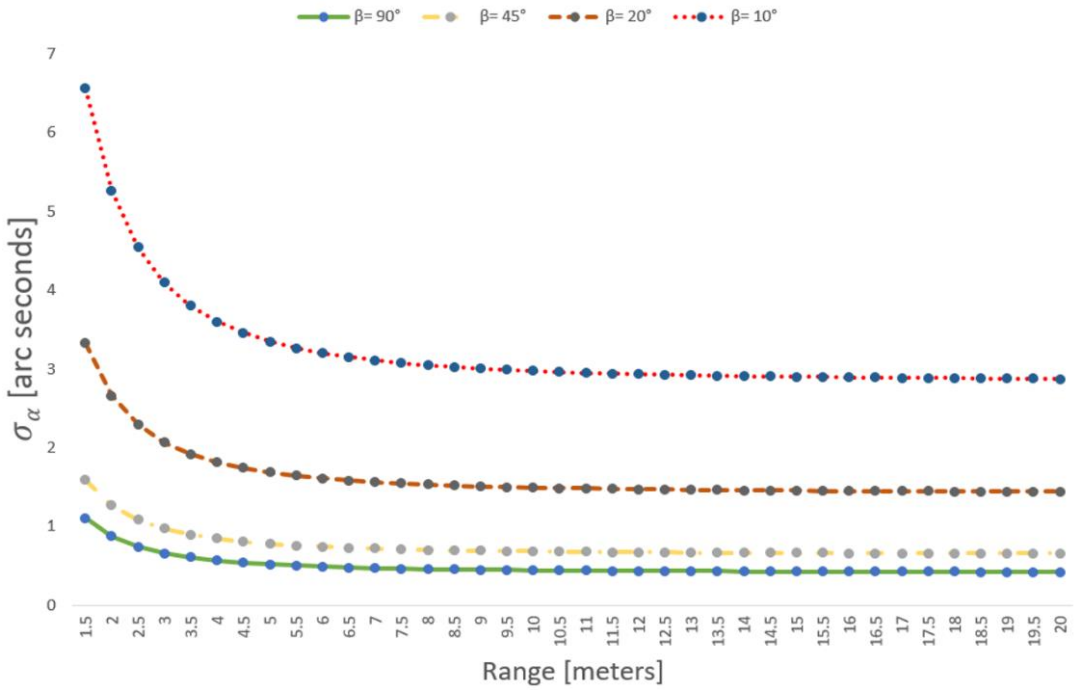

Fig. 4. *Modeled a priori σ_α values (Eq. 9) at varying zenith angles (β) for a Leica AT400 series laser tracker (a = 22 µm, b = 6 µm/m, $\sigma_L = 0.5$")*

Fig. 5 does the same for a FARO Vantage laser tracker given the following published ASME standard transverse MPE values: $A_T = 20\ \mu m,\ B_T = 5\ \mu m/m$ (FARO Technologies, Inc., 2016).

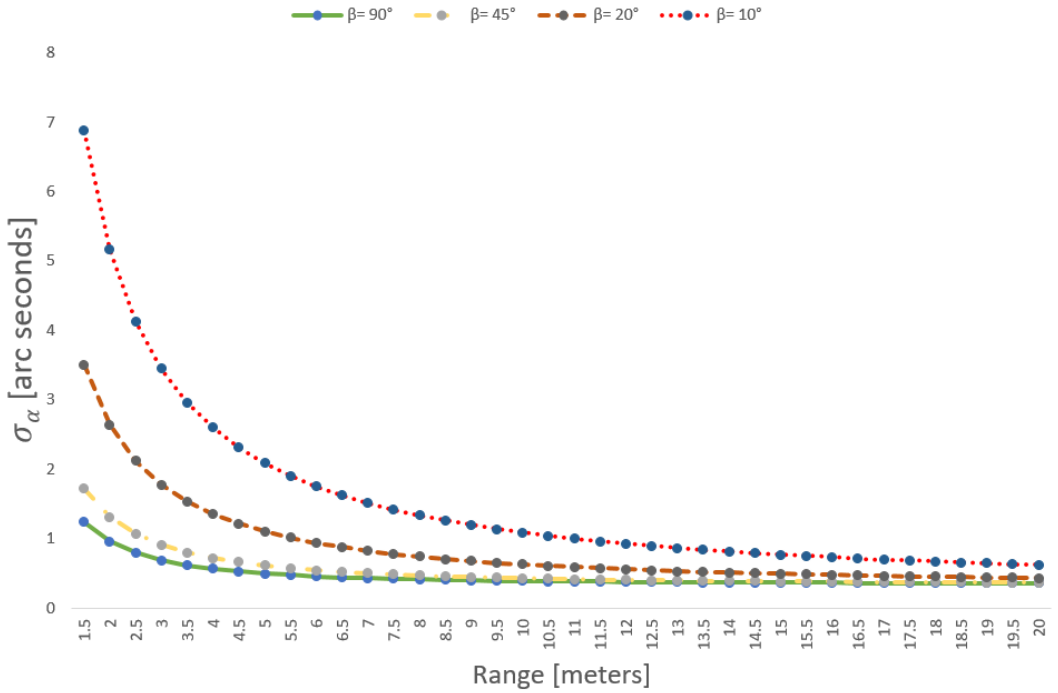

Fig. 5. *Modeled a priori σ_α values (Eq. 9) at varying zenith angles (β) for a FARO Vantage series laser tracker (a = 26 µm, b = 5 µm/m, $\sigma_L = N/A$)*

The Leica and FARO trackers have comparable a and b values, but the plots in Fig. 4 and Fig. 5 are noticeably different because the FARO tracker does not apply leveling compensations to the raw angular measurements (so the σ_L term is not applicable). For the FARO tracker in Fig. 5, the uncertainty of azimuth angles at all four zenith angles converge to roughly 0.5 arcseconds at the far range because σ_R is dominant at the far range while uncertainties from transverse offset errors become insignificant. The plot for the Leica tracker in Fig. 4 does not have the same convergence of azimuthal uncertainty at the far ranges because σ_L becomes the dominant source of error for steep measurements at the far ranges. Fig. 4 and Fig. 5 demonstrate that correctly modeling uncertainties of azimuth angles as a function of range and zenith angle is especially significant for steep sightings and at near ranges.

This paper's proposed modeling of the uncertainty of azimuth and zenith angles (Eqs. 8 and 9) suggests using the MPE angular performance values published by the manufacturer as a starting point. There are limitations to modeling angular uncertainty in this way; no two laser trackers are the same even if each is the same model as the other and made by the same manufacturer. The performance values can be refined to reflect the actual performance of a particular laser tracker. The repetition of measurements is a good way to empirically refine a and b values for a pairing of a particular laser tracker and SMR. Chapter 4 of *Precision Surveying: The Principles and Geomatics Practice* by John Ogundare describes detailed procedures to determine the pointing accuracy (σ_P) and reading accuracy (σ_R) using the repetition method (Ogundare, 2015).

A similar modeling of the azimuth angle uncertainty was proposed by John W. Dorsey-Palmateer in the Journal of the CMSC (Dorsey-Palmateer, 2018). The article implies that σ_α should be equivalent to $\sigma_\beta / \sin(\beta)$ for calculating Monte Carlo simulated uncertainty volumes for the coordinates of measured points. This insight is on the right track, but it does not take into account one important consideration; only a portion of the angular uncertainty in an azimuth angle should be divided by $\sin(\beta)$ because the uncertainty of the horizontal angular encoder reading (σ_R) is unaffected by how steep the measurement is. Also, the article does not consider errors that may be present from leveling compensation or address how to relate MPE angular performance values reported from laser tracker manufacturers to determine a

priori angular uncertainties. By taking into account the physical underlying principles of the error sources, this paper proposes refining the simplistic assumption that $\sigma_\alpha = \sigma_\beta / \sin(\beta)$ and instead only applies the sine term to the a value and not to the b value as reflected in Eq. 9.

Repeatability Test

A simple repeatability test was done using a recently calibrated Leica AT402 laser tracker and a FARO Vantage laser tracker to demonstrate that azimuth angles become less accurate with increased steepness. The SMR used was certified to have an optical centering of ± 3 µm and sphericity of ± 3 µm. Four SMR positions were each measured 20 times in both faces (front sight and back sight modes) as shown in Fig. 6.

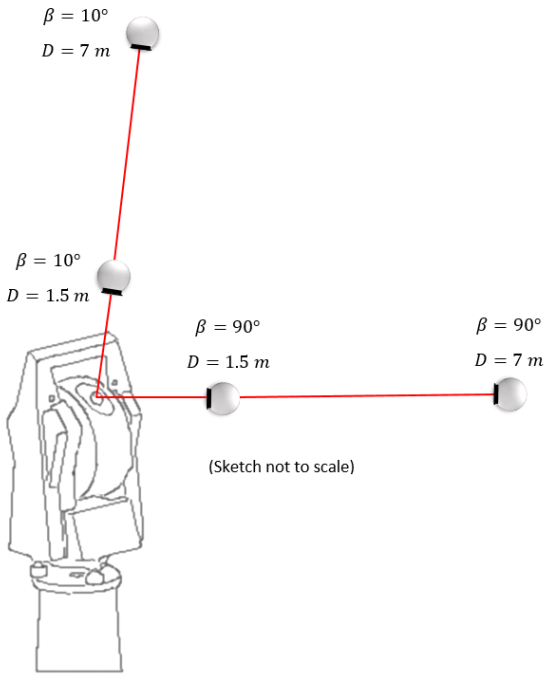

Fig. 6. *Angular repeatability tests at four SMR positions*

For the Leica AT402, the measurements were taken with the inclinometer applying leveling compensations to the angular measurements. The measurements were taken at β = 10° and β = 90° with ranges of 1.5 meters and 7 meters. After each measurement, the SMR was rotated 90° in its nest about the line of sight to vary the offset direction of any optical centering errors in the SMR.

Table 1 shows the sample standard deviations of the 20 azimuth and zenith angles from the Leica AT402 and FARO Vantage laser trackers after averaging the front sight and back sight values.

Table 1. *Sample standard deviations of azimuth and zenith measurements at 4 SMR positions*

Laser Tracker	*Zenith*	σ_α *@ D = 1.5 (m)*	σ_β *@ D = 1.5 (m)*	σ_α *@ D = 7 (m)*	σ_β *@ D = 7 (m)*
Leica AT402	β = 10°	σ_α = 10.8"	σ_β = 0.7"	σ_α = 7.5"	σ_β = 0.4"
Leica AT402	β = 90°	σ_α = 0.4"	σ_β = 0.7"	σ_α = 0.2"	σ_β = 0.3"
FARO Vantage	β = 10°	σ_α = 5.3"	σ_β = 1.0"	σ_α = 2.3"	σ_β = 0.9"
FARO Vantage	β = 90°	σ_α = 0.2"	σ_β = 0.3"	σ_α = 0.3"	σ_β = 0.3"

The values in Table 1 show that the sample standard deviation between azimuth and zenith angles are comparable to each other at β = 90°. However, the azimuth angles were much less repeatable when viewed more steeply.

The purpose of this paper's repeatability test is to empirically demonstrate that steepness and range have a noticeable effect on the accuracy of the azimuth angle. The repeatability test is not meant to directly verify the true accuracy of the laser tracker—that is what the ISO and ASME standards are for. The repeatability of measurements only represents the rough magnitude of random errors under nearly identical conditions and can only loosely imply the actual size of random errors. Repeatability tests also say nothing about the size of systematic errors that may be present (such as biases, offsets, etc.) (Ridler, Lee, Martens, & Wong, 2007). Other papers, such as by Muralkrishnan et al., discuss methods for detecting and correcting systematic laser tracker angular measurements (Muralkrishnan, et al., 2010).

Spherical to Cartesian Transformation

Propagating laser tracker observation uncertainties $\sigma_D, \sigma_\alpha, \sigma_\beta$ to coordinate values X, Y, Z of measured points through the spherical-to-Cartesian transformation reveals their impact on $\sigma_X, \sigma_Y, \sigma_Z$. Given a laser tracker measurement where $D = \text{Slope Distance}$, $\alpha = \text{Azimuth Angle}$, $\beta =$

Zenith Angle as shown in Fig. 7, the spherical-to-Cartesian coordinate transformation equations are the following:

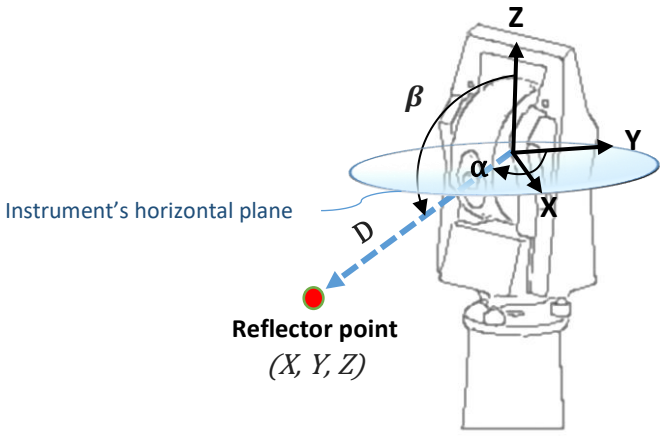

Fig. 7. *Spherical to Cartesian transformation*

$$X = D\ sin(\alpha)\ sin(\beta) \tag{10a}$$

$$Y = D\ cos(\alpha)\ sin(\beta) \tag{10b}$$

$$Z = D\ cos(\beta) \tag{10c}$$

Error Propagation

Eqs. 11 through 16 show the steps to calculating $\sigma_X, \sigma_Y, \sigma_Z$ from $\sigma_D, \sigma_\alpha, \sigma_\beta$.

Putting Eqs. 10a, 10b, and 10c in matrix form:

$$\begin{bmatrix} f_X(D,\alpha,\beta) \\ f_Y(D,\alpha,\beta) \\ f_Z(D,\alpha,\beta) \end{bmatrix} = \begin{bmatrix} X \\ Y \\ Z \end{bmatrix} = \begin{bmatrix} D\ sin(\alpha)\ sin(\beta) \\ D\ cos(\alpha)\ sin(\beta) \\ D\ cos(\beta) \end{bmatrix}$$

Given a variance matrix of observations D, α, β:

$$\boldsymbol{\Sigma} = \begin{bmatrix} {\sigma_D}^2 & 0 & 0 \\ 0 & {\sigma_\alpha}^2 & 0 \\ 0 & 0 & {\sigma_\beta}^2 \end{bmatrix} \tag{11}$$

A Jacobian matrix of partial derivatives:

$$\boldsymbol{J} = \begin{bmatrix} \frac{\partial f_X}{\partial D} & \frac{\partial f_X}{\partial \alpha} & \frac{\partial f_X}{\partial \beta} \\ \frac{\partial f_Y}{\partial D} & \frac{\partial f_Y}{\partial \alpha} & \frac{\partial f_Y}{\partial \beta} \\ \frac{\partial f_Z}{\partial D} & \frac{\partial f_Z}{\partial \alpha} & \frac{\partial f_Z}{\partial \beta} \end{bmatrix} = \begin{bmatrix} sin(\alpha)\ sin(\beta) & D\ cos(\alpha)\ sin(\beta) & D\ sin(\alpha)\ cos(\beta) \\ cos(\alpha)\ sin(\beta) & -D\ sin(\alpha)\ sin(\beta) & D\ cos(\alpha)\ cos(\beta) \\ cos(\beta) & 0 & -D\ sin(\beta) \end{bmatrix} \tag{12}$$

Apply principles of error propagation:

$$\begin{bmatrix} {\sigma_X}^2 & \sigma_X\sigma_Y & \sigma_X\sigma_Z \\ \sigma_X\sigma_Y & {\sigma_Y}^2 & \sigma_Y\sigma_Z \\ \sigma_X\sigma_Z & \sigma_Y\sigma_Z & {\sigma_Z}^2 \end{bmatrix} = \boldsymbol{J}\,\boldsymbol{\Sigma}\,\boldsymbol{J}^{\boldsymbol{T}} \tag{13}$$

Solving for $\sigma_X, \sigma_Y, \sigma_Z$

$$\sigma_X = \sqrt{D^2{\sigma_\alpha}^2\cos(\alpha)^2\sin(\beta)^2 + D^2{\sigma_\beta}^2\cos(\beta)^2\sin(\alpha)^2 + {\sigma_D}^2\sin(\alpha)^2\sin(\beta)^2} \tag{14}$$

$$\sigma_Y = \sqrt{D^2{\sigma_\alpha}^2\sin(\alpha)^2\sin(\beta)^2 + D^2{\sigma_\beta}^2\cos(\alpha)^2\cos(\beta)^2 + {\sigma_D}^2\cos(\alpha)^2\sin(\beta)^2} \tag{15}$$

$$\sigma_Z = \sqrt{D^2{\sigma_\beta}^2\sin(\beta)^2 + {\sigma_D}^2\cos(\beta)^2} \tag{16}$$

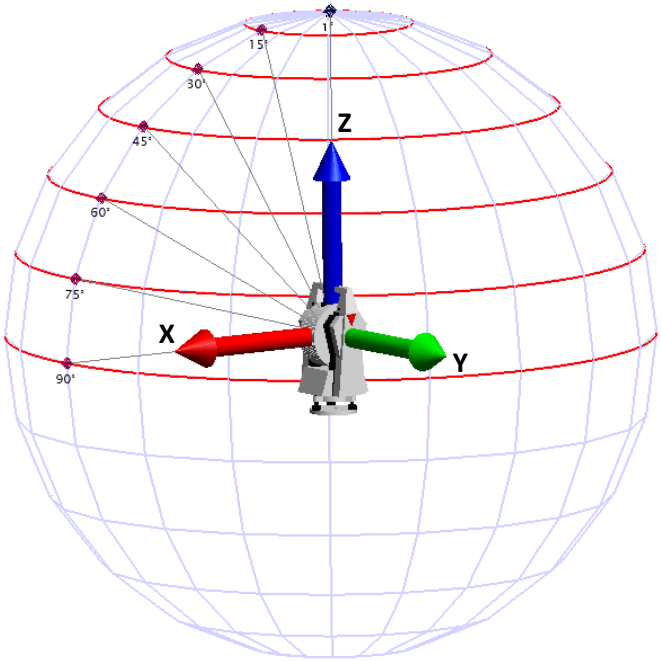

Fig. 8. *Simulated measurements at a 1.5 (m) range and varying zenith angles*

Using Eqs. 14 - 16, it can be shown that the commonly used stochastic model of $\sigma_\alpha = \sigma_\beta$ does not make sense at steep angles. Applying a stochastic model of $\sigma_\alpha = \sigma_\beta = 1$" to calculate $\sigma_X, \sigma_Y, \sigma_Z$ for 7 simulated points, each measured at a 1.5 meter range and spaced apart by 15° vertically in the XZ plane, shows the flaw of this stochastic approach.

Table 2 shows the results of applying the error propagation of the $\sigma_\alpha = \sigma_\beta = 1"$ stochastic model to the simulated measurements shown in Fig. 8.

***Table 2**. Error propagation from observations $(\sigma_\beta, \sigma_\alpha, \sigma_D)$ to coordinates $(\sigma_X, \sigma_Y, \sigma_Z)$ where $\sigma_D = 10$ µm and $\sigma_\alpha = \sigma_\beta = 1"$ (a common and simplistic, yet flawed stochastic model)*

β	α	D	σ_β	σ_α	σ_D	X	Y	Z	σ_X	σ_Y	σ_Z
1°	90°	1.5 m	1"	1"	10 µm	0.026179 m	0.000000 m	1.499772 m	7 µm	**0 µm**	10 µm
15°	90°	1.5 m	1"	1"	10 µm	0.388229 m	0.000000 m	1.448889 m	7 µm	2 µm	10 µm
30°	90°	1.5 m	1"	1"	10 µm	0.750000 m	0.000000 m	1.299038 m	8 µm	4 µm	9 µm
45°	90°	1.5 m	1"	1"	10 µm	1.060660 m	0.000000 m	1.060660 m	9 µm	5 µm	9 µm
60°	90°	1.5 m	1"	1"	10 µm	1.299038 m	0.000000 m	0.750000 m	9 µm	6 µm	8 µm
75°	90°	1.5 m	1"	1"	10 µm	1.448889 m	0.000000 m	0.388229 m	10 µm	7 µm	7 µm
90°	90°	1.5 m	1"	1"	10 µm	1.500000 m	0.000000 m	0.000000 m	10 µm	7 µm	7 µm

Notice that Table 2 shows $\sigma_Y = 0\ \mu m$ for the near-vertical measurement at $\beta = 1°$. (highlighted). A value of $\sigma_Y = 0$ is not realistic because there should be at least several micrometers of lateral uncertainty present outside of the XZ plane from azimuthal pointing and target errors that should be represented in the Y dimension. This demonstrates that $\sigma_\alpha = \sigma_\beta$ is not a good stochastic model for steep measurements.

Table 3 shows the error propagation of the same simulated measurements in Table 2, but using the stochastic model proposed by this paper in Eqs. 8 and 9, assuming no leveling compensation, and using a = 22 µm and b = 5 µm/m. This model only holds $\sigma_\alpha = \sigma_\beta = 1"$ at $\beta = 90°$.

***Table 3**. Error Propagation from observations $(\sigma_\beta, \sigma_\alpha, \sigma_D)$ to coordinates $(\sigma_X, \sigma_Y, \sigma_Z)$ where σ_D =10 µm and σ_α and σ_β are determined by Eq. 8 and Eq. 9 using a = 22 µm and b = 5 µm/m*

β	α	D	σ_β	σ_α	σ_D	X	Y	Z	σ_X	σ_Y	σ_Z
1°	90°	1.5 m	1"	58"	10 µm	0.026179 m	0.000000 m	1.499772 m	7 µm	**7 µm**	10 µm
15°	90°	1.5 m	1"	3.9"	10 µm	0.388229 m	0.000000 m	1.448889 m	7 µm	7 µm	10 µm
30°	90°	1.5 m	1"	2.0"	10 µm	0.750000 m	0.000000 m	1.299038 m	8 µm	7 µm	10 µm
45°	90°	1.5 m	1"	1.5"	10 µm	1.060660 m	0.000000 m	1.060660 m	9 µm	8 µm	9 µm
60°	90°	1.5 m	1"	1.2"	10 µm	1.299038 m	0.000000 m	0.750000 m	9 µm	8 µm	8 µm
75°	90°	1.5 m	1"	1.1"	10 µm	1.448889 m	0.000000 m	0.388229 m	10 µm	8 µm	7 µm
90°	90°	1.5 m	1"	1"	10 µm	1.500000 m	0.000000 m	0.000000 m	10 µm	9 µm	7 µm

Table 3 shows $\sigma_Y = 7\ \mu m$ for the near vertical measurement at $\beta = 1°$ by weighting $\sigma_\alpha = 58"$ (highlighted). The σ_Y values in Table 3 are more realistic than the near-zero σ_Y values in Table 2. This

demonstrates that Eq. 9 better models the uncertainty of azimuth observations for steep and near-range measurements than more simplistic modeling approaches.

Conclusion

In this paper, a unique approach to modeling a priori uncertainties of laser tracker angle measurements based on manufacturers' reported MPE performance values was proposed in detail. This approach takes into account the various sources of a spherical instrument's angular errors and how they propagate to the measured coordinates of a point. A field test of laser tracker repeatability and simulated measurement scenarios were presented to demonstrate that the proposed modeling approach provides realistic results and is consistent with observable effects in real-world measurements.

Data Availability Statement

Some of the data that supports the findings of this study are available from the corresponding author upon reasonable request, including the repeatability test angle measurements.

Acknowledgments

This material is based upon work supported by the U.S. Department of Energy, Office of Science, Office of Nuclear Physics and used resources of the Facility for Rare Isotope Beams (FRIB), which is a DOE Office of Science User Facility, operated by Michigan State University, under Award Number DE-SC0000661. The author would like to thank Luke Privatte for taking hundreds of measurements with the Leica AT402 and Vantage laser trackers for the repeatability test. Also, thanks to Doug Bruce for providing useful input during the writing of this paper. Finally, thanks to the reviewers who provided detailed comments to improve the content of this paper.

References

Anderson, J. M., & Mikhail, E. M. (1998). *Surveying Theory and Practice.* Boston: WCB/McGraw-Hill.

ASME. (2006). *ASME B89.4.19 Performance Evaluation of Laser-Based Spherical Coordinate Measurement Systems.* New York: The American Society of Mechanical Engineers.

Dorsey-Palmateer, J. W. (2018). A New Model for Spherical Instrument Measurement Uncertainty. *The Journal of the CMSC*, 18-23.

FARO Technologies, Inc. (2016). *FARO laser tracker vantage user manual April 2016.*

Ghilani, C. D. (2010). *Adjustment computations spatial data analysis. 5th ed.* Hoboken, NJ: John Wiley & Sons.

Ghilani, C. D. (2016, April). A correctly weighted least squares adjustment part 3, estimating standard errors in angular observations. *xyHt*, pp. 44-45.

Hexagon Metrology. (2012). *Leica Absolute Tracker AT401 Product Brochure.* Hexagon Metrology.

Hexagon Metrology. (2018). *Leica Absolute Tracker AT403 ASME B89.4.19-2006 Specifications.* Hexagon Metrology.

Hexagon Metrology. (2021). *SpatialAnalzer User Manual.* Williamsburg: Hexagon Metrology.

ISO. (2021). *Geometrical product specifications (GPS) — Acceptance and reverification tests for coordinate measuring systems (CMS) — Part 10: Laser trackers.* Geneva: International Organization for Standardization.

Leica Geosystems. (2009, January). *Leica TDRA6000 Product Brochure Version 01/2009.* Retrieved from www.geowild.hr: https://www.geowild.hr/wp-content/uploads/digital_products/leica%20tdra6000%20brochure_en.pdf

Leica Geosystems. (2010, March 24). *Leica_Absolute_Tracker_AT401_white_paper.pdf.* Unterentfelden: Leica Geosystems. Retrieved from leica-geosystems.com/metrology: https://www.swisstek.com/images/wild_leica/Leica_Absolute_Tracker_AT401_white_paper.pdf

Manwiller, P. E. (2020). Three-Dimensional Network Adjustment of Laser Tracker Measurements for Large-Scale Metrology Applications. *Journal of Surveying Engineering*.

Meid, A., & Sandwith, S. (2000). Dynamic Weighting of Laser Tracker Measurements for Bundle Adjustment. *Proceedings of the Boeing Large Scale Optical Metrology Seminar.* Long-Beach, CA.

MetrologyWorks. (2022, June 21). Retrieved from www.metrologyworks.com: https://www.metrologyworks.com/wp-content/uploads/SMR.pdf

Muralikrishnan, B., Sawyer, D., Blackburn, C., Phillips, S., Borchardt, B., & Estler, W. (2009, Jan-Feb). ASME B89.4.19 Performance Evaluation Tests and Geometric Misalignments in Laser Trackers. *Journal of Research of the National Institute of Standards and Technology*, 21-35.

Muralkrishnan, B., Blackburn, C., Sawyer, D., & Phillips, S. (2010). Measuring scale errors in a laser tracker's horizontal angle encoder through simple length measurement and two-face systems tests. *Journal of Research of the National Institute of Standards and Technology*, 291-301.

Ogundare, J. O. (2015). *Precision Surveying: The Principles and Geomatics Practice.* Hoboken: John Wiley & Sons.

Ridler, N., Lee, B., Martens, J., & Wong, K. (2007). Measurement Uncertainty, Traceability, and the GUM. *IEEE Microwave Magazine*, 44-53.

Thompson, A., Southon, N., Florian, F., Stupfler, G., & Leach, R. (2021). Efficient empirical determination of maximum permissible error in coordinate metrology. *Measurement Science and Technology*.

Ulrich, T. (2016). *Uncertainty Modelling of High-precision Trajectories.* Karlsruhe, Germany: Karlsruher Institut für Technologie.

Wang, L., Muralikrishnan, B., Hernandez, O. I., Shakarji, C., & Sawyer, D. (2020). Performance evaluation of laser trackers using the network method. *Measurement*, 108165.